

## Error Growth in Flows with Finite-Amplitude Waves or Coherent Structures

C. SNYDER

*National Center for Atmospheric Research,\* Boulder, Colorado*

(Manuscript received 6 May 1997, in final form 20 March 1998)

### ABSTRACT

Explanations of error growth in atmospheric flows are often based on the extension of barotropic and baroclinic instabilities from steady parallel flows to weakly nonparallel and time-dependent flows. Consideration of simple flows with finite-amplitude waves, however, suggests an additional scenario for error growth: an initial error that changes the wave amplitude or the medium through which the wave propagates will alter the propagation of the wave and result in a growing phase error. This scenario is illustrated and generalized to other coherent structures through several examples for which analytic solutions are available. For a basic state of a barotropic Rossby wave, growing phase errors account for the most rapidly growing disturbances over time intervals long compared to the basic-state advective timescale; over shorter intervals, amplifications of phase errors are smaller than, but comparable to, the optimal amplification. The role of this mechanism in forecast error growth is less certain, but its importance is suggested by the fact that short-range forecast errors are typically errors in the position or intensity of existing features.

### 1. Introduction

Knowledge of error growth, or more generally the growth of small perturbations, in complex time-dependent flows is crucial to questions of predictability and the origin of forecast error, and it is relevant as well to dynamical problems such as cyclogenesis. At scales resolved in current global forecast models, the fastest growing errors often grow through mechanisms familiar from studies of finite-time baroclinic or barotropic instability of steady parallel flows (Farrell 1985, 1989; Buizza and Palmer 1995). Such instabilities are typically modulated by, but do not require, finite-amplitude waves or other spatial variations within the basic-state flow (e.g., Borges and Hartman 1992). These analogs of baroclinic and barotropic instabilities, however, cannot explain all instances of rapid error growth within realistic atmospheric flows (Buizza and Palmer 1995; Snyder and Joly 1998).

The present paper explores an alternative mechanism for error growth that relies on the presence of waves or other finite-amplitude features in the flow. In its simplest form, this mechanism results in a growing error in the position of these preexisting features. Consider, for ex-

ample, a flow that contains a finite-amplitude wave. The phase speed of such a wave will depend on its amplitude and on properties of the medium through which it propagates. Perturbations that change the medium or the wave amplitude will therefore alter the propagation of the wave and an error in the position, or phase, of the wave will grow. (The ideas presented here are most relevant to error growth, but we will often for convenience adopt the terminology of stability theory and discuss basic states and perturbations.) If both the original and perturbed waves move with constant (but different) phase speeds, the growth will be linear in time for sufficiently small errors.

Although this simple scenario results in a growing phase error for a finite-amplitude wave, the same conceptual and mathematical framework is applied below to examples of errors in the position of other coherent structures, or in the amplitude of such structures, or in the growth rate of growing or decaying features. Thus, the term "phase error" will be used in a general sense, referring to errors in the position, orientation, amplitude, or growth of preexisting features in the flow. Most stability analyses applied to error growth, in contrast, predict the appearance of qualitatively new structure, such as the development of baroclinic waves on a smooth zonal jet.

The notion that forecast errors often consist of errors in the position and intensity of existing features is hardly controversial. [For supporting evidence, see, e.g., Figs. 2–4 of Hawes and Colucci (1986).] Nor is it novel to suggest that small initial errors in the position or inten-

---

\* The National Center for Atmospheric Research is sponsored by the National Science Foundation.

---

Corresponding author address: Dr. Chris Snyder, NCAR, P.O. Box 3000, Boulder, CO 80307-3000.  
E-mail: chriss@ncar.ucar.edu

sity of existing features, or errors in the advecting flow, will give rise to larger errors in subsequent forecasts. Theoretical investigations, however, typically have not emphasized the relation between growing errors and preexisting features in the flow, and instead have approached error growth as a generalization of barotropic–baroclinic instabilities of steady parallel flows.

The growth of phase errors will be examined in several simple examples for which analytic solutions are available for both the basic state and specific classes of initial perturbations. First, we will return to a finite-amplitude wave as a basic state, examining the barotropic Rossby wave in section 2. Results are shown to be relevant to the most rapidly growing finite-time perturbations for the same basic state, as calculated by Yoden and Nomura (1993). Section 3 presents generalizations to baroclinic edge waves, to barotropic waves on a circular patch of vorticity, and to growing or decaying waves. A basic state consisting of a barotropic vortex dipole is considered in section 4. In each of these examples, the perturbations increase algebraically in  $t$  and clearly represent phase errors in the sense defined above. Relevance to the growth of errors in more complex flows is argued in the final section.

## 2. Perturbations to a barotropic Rossby wave

The evolution of nondivergent barotropic flow on a  $\beta$  plane is governed by

$$\zeta_t + J(\psi, \zeta + \beta y) = 0, \quad (1)$$

where the streamfunction  $\psi$  is related to the velocity by  $(u, v) = (-\psi_y, \psi_x)$  and  $\zeta = \nabla^2 \psi$  is the vorticity. We seek finite-amplitude solutions to (1) of the form  $\bar{\psi} = P(x - \bar{c}t, y)$ , that is, a steadily propagating solution with zonal phase speed  $\bar{c}$ . The overbar indicates that this solution will be used subsequently as a basic state.

In the translating coordinates  $\hat{x} = x - \bar{c}t$ ,  $\hat{y} = y$ ,  $\hat{t} = t$ , (1) requires

$$J(P + \bar{c}\hat{y}, \nabla^2 P + \beta\hat{y}) = 0,$$

which is satisfied if  $\nabla^2 P = -\kappa^2 P$  and  $\bar{c} = -\beta/\kappa^2$ . Thus, a solution of the desired form is

$$\bar{\psi} = \bar{\psi}_0 \cos k(x - \bar{c}t) \sin ly, \quad (2)$$

with  $\bar{\psi}_0$  an arbitrary amplitude and  $\bar{c} = -\beta/(k^2 + l^2)^{-1}$ .

Sufficiently small perturbations  $\psi'$  satisfy the linearized form of (1):

$$\zeta'_t + J(\bar{\psi}, \zeta') + J(\psi', \bar{\zeta} + \beta y) = 0, \quad (3)$$

where  $\zeta' = \nabla^2 \psi'$ . Suppose that the initial perturbation consists of a zonal flow,

$$\psi'(x, y, 0) = -u'_0 y. \quad (4)$$

It is then straightforward to check that the subsequent evolution is given by

$$\begin{aligned} \psi'(x, y, t) &= u'_0(-y - t\bar{\psi}_x) \\ &= u'_0[-y + k\bar{\psi}_0 t \sin k(x - \bar{c}t \sin ly)]. \end{aligned} \quad (5)$$

The time-dependent part of  $\psi'$  thus increases linearly with  $t$ , propagates at the same speed as  $\bar{\psi}$ , and has structure identical to that of  $\bar{\psi}$  but phase-shifted zonally by a quarter wavelength. In addition, the amplitude of the time-dependent part of  $\psi'$  is proportional to  $\bar{\psi}_0$ , the amplitude of the basic-state wave.

The timescale  $\tau$  for the growth of  $\psi'$  should scale as the time required for the bracketed terms in (5) to become comparable. If the basic-state wave fills the domain meridionally ( $y \sim l^{-1}$ ) and the zonal and meridional scale are comparable ( $l \sim k$ ), then

$$\tau \sim (k^2 \bar{\psi}_0)^{-1}. \quad (6)$$

Thus, the perturbation develops on the advective timescale from the basic state. For this example,  $\tau$  is also the timescale for shear instabilities, whose growth rates scale as the local basic-state shear. In the case of the baroclinic edge wave that follows, however, the distinction between  $\tau$  and timescales for shear instabilities will be clear.

The evolution of  $\psi'$  is hardly surprising. A perturbation to the zonal mean flow, even of finite amplitude, simply changes the phase speed of the basic-state wave from  $\bar{c}$  to  $\bar{c} + u'_0$ . The difference between these two finite-amplitude solutions is periodic in time and can be written as

$$-u'_0 y + 2\bar{\psi}_0 \sin\left(\frac{1}{2}ku'_0 t\right) \sin\left[kx - k\left(\bar{c} + \frac{1}{2}u'_0\right)t\right] \sin ly.$$

The linearized solution (5) is then valid for short times or small  $u'_0$  satisfying  $ku'_0 t \ll 1$ .

Although  $\bar{\psi}$  is a finite-amplitude, fully nonlinear solution of (1), it is worth noting that a basic state consisting of a small-amplitude linear wave would also support perturbations of the form (5). Growth in that case, however, would be correspondingly slow, since  $\tau$  scales as  $\bar{\psi}_0$ . Significant growth therefore requires a basic-state wave of finite amplitude, even though nonlinearity of the basic-state dynamics is not essential. Basic states with nonlinear dynamics also support a larger variety of perturbations that lead to growing phase errors; the propagation of nonlinear waves, for example, may depend on their amplitude, as in the example below of waves on a barotropic vortex.

Comparison of the growing phase error (5) with other barotropic instabilities, both exponential and finite time, is instructive.

The energetic budget associated with (5) is similar to other barotropic instabilities; the growth of the perturbation kinetic energy is associated with conversion of the basic-state kinetic energy. An important difference from the usual case is that this conversion is accomplished *without* the perturbation having horizontal phase tilts. Unfortunately, it is not clear how to use this dif-

ference to distinguish perturbations that grow as phase errors, particularly in less idealized examples.

Direct comparison can also be made with the results of Yoden and Nomura (1993, YN hereafter), who calculate the most rapidly growing perturbations to the basic state (2) for various time intervals. They use a truncated spectral model and measure the perturbation amplitude in the  $L_2$ , or streamfunction squared, norm. Although (5) is not an exact solution in their model (because of the truncation and because the perturbation velocity is required to be zero at  $y = 0, n\pi/l$ ), their model does support an analogous solution of the form

$$\psi' = u'_0(\eta(y) + t\bar{\psi}_x), \quad (7)$$

which represents a phase shift of the basic-state wave that grows linearly with time. Details are given in the appendix.

Calculation of amplifications from (7) and comparison with YN shows that the growth of this perturbation is not optimal for time intervals  $\Delta t$  comparable to or shorter than  $\tau = (k^2\bar{\psi}_0)^{-1}$ . For example, using  $l = k$  and  $\bar{\psi}_0 = 2.5\beta/k^3$  as in YN, the square root of the  $L_2$  norm of (7) amplifies by a factor of 3 when  $\Delta t = 3.5\tau$ , while the optimal amplification is slightly greater than 7 (see Fig. 9 in YN;  $\Delta t = 3.5\tau$  corresponds to  $\tau = 6$  in their notation).

For longer time intervals, however, (7) agrees well with YN's results. They find<sup>1</sup> that the optimal amplification is bounded by  $0.89\Delta t/\tau$  for  $\Delta t/\tau \gg 1$ ; the amplification of (7) is asymptotically  $0.83\Delta t/\tau$ . This agreement indicates that the perturbation growth for times long compared to  $(k^2\bar{\psi}_0)^{-1}$  is dominated by a phase shift of the basic-state wave.

### 3. Other basic states with finite-amplitude waves

We examine next three additional examples in which the basic state contains finite-amplitude waves. In the first, the basic state is a baroclinic quasigeostrophic edge wave. Perturbing the surface temperature gradient on which this wave propagates leads to a growth of phase errors much as for the barotropic Rossby wave above. The second example illustrates the growth of errors in the phase of barotropic waves on a patch of vorticity. In this case, we derive the behavior of certain perturbations through a Taylor expansion of the dispersion relation for the basic-state wave. The final example generalizes the Taylor-expansion technique to growing basic-state waves.

<sup>1</sup> Their Fig. 10 shows that the quantity  $\alpha(t)$  is linear in time:  $\alpha(t)$ , given by their (11), is the rms amplification of random perturbations that are initially Gaussian, independent, and of identical variance in each of the model's  $N$  degrees of freedom. The maximum amplification is then bounded above by  $N^{1/2}\alpha(t)$ .

#### a. Baroclinic edge wave

Consider a Boussinesq quasigeostrophic zonal flow on an  $f$  plane, with uniform vertical shear  $\Lambda$ , corresponding meridional potential temperature gradient  $-f\theta_0\Lambda/g$ , and buoyancy frequency  $N^2$ . Disturbances to this flow that have uniform pseudo-potential vorticity satisfy

$$\psi_{xx} + \psi_{yy} + (f^2/N^2)\psi_{zz} = 0$$

and evolve according to the conservation of potential temperature at the surface,

$$\psi_{zt} + J(\psi, \psi_z - \Lambda y) = 0 \quad \text{at } z = 0. \quad (8)$$

Here,  $\psi$  is the geostrophic streamfunction and potential temperature is given by  $(f\theta_0/g)\psi_z$ . The flow is assumed unbounded above, requiring  $\psi$  to be bounded as  $z \rightarrow \infty$ . Further details are given in Gill (1982, section 13.2).

Following the technique outlined in section 2, nonlinear wave solutions may be found of the form

$$\bar{\psi}(x, y, z, t) = \bar{\psi}_0 \cos k(x - \bar{c}t) \sin ly \exp(-N\kappa z/f), \quad (9)$$

where  $\bar{c} = f\Lambda/N\kappa$  and  $\kappa = (k^2 + l^2)^{1/2}$ . If (8) is linearized about  $\bar{\psi}$ , an initial perturbation to the background vertical shear,

$$\psi'(x, y, z, 0) = -\Lambda'yz, \quad (10)$$

then evolves as

$$\begin{aligned} \psi' = \Lambda'[-yz + (fk/N\kappa)\bar{\psi}_0 t \sin k(x - \bar{c}t) \\ \times \sin ly \exp(-N\kappa z/f)]. \end{aligned} \quad (11)$$

As in the barotropic solution (5), the perturbation has amplitude increasing as  $\bar{\psi}_0 t$ , has the same phase speed as  $\bar{\psi}$ , and shares the spatial structure of  $\bar{\psi}$  except for a phase shift of one-quarter wavelength. The perturbation dynamics in this case, however, are more substantive than simply altering the frame of reference. The initial perturbation modifies the zonal shear and thus the surface temperature gradient on which the basic-state wave propagates.

Also as in the barotropic solution, the time  $\tau$  required for the bracketed terms in (11) to become comparable is given by (6):  $\tau \sim (k^2\bar{\psi}_0)^{-1}$ , again assuming that  $ly \sim 1$  and  $l \sim k$  and now scaling height by the Rossby depth ( $N\kappa z/f \sim 1$ ). Thus,  $\tau$  is again the basic-state advective time and is independent of  $f$ ,  $N$ , and, in particular, the background baroclinic shear  $\Lambda$ . Finite-time instabilities of the baroclinic shear (10) without a superposed wave would, in contrast, have amplifications that scale as  $f\Lambda/N$ .

Finally, it is worth noting that the energetic budget for  $\psi'$  is indistinguishable from a mixed barotropic-baroclinic instability. Both baroclinic and barotropic conversions contribute to the growth of total perturbation energy and, in fact, are equal, although the perturbation has no phase tilts in the traditional sense, as was the case for (5).

*b. Waves on a barotropic circular vortex*

A localized barotropic vortex supports Rossby waves that propagate on the vorticity gradients along the vortex edge. The simplest example, which will be considered here, is a circular vortex of constant interior vorticity  $\bar{\zeta}$  and zero external vorticity. The linear waves supported by this vortex are discussed by Lamb (1945, art. 158).

Analytic solutions for finite-amplitude waves are available for azimuthal wavenumber 2 (see Lamb 1945, art. 159). These solutions have the form of an elliptical vortex with axes of length  $a$  and  $b$  and rotating at constant frequency  $\bar{n}$ , given by

$$\bar{n} = \frac{ab}{(a + b)^2} \bar{\zeta}. \tag{12}$$

In elliptic cylindrical coordinates  $(\xi, \eta)$ , the streamfunction external to the vortex is

$$\bar{\psi} = \frac{1}{4} ab \bar{\zeta} (2\xi + e^{-2\xi} \cos 2\eta), \tag{13a}$$

where

$$d \cosh \xi \cos \eta = x, \quad d \sinh \xi \sin \eta = y, \tag{14}$$

and  $d = (a^2 - b^2)^{-1/2}$ . The elliptical boundary of the vortex is given by  $\cosh \xi = a/d$ . In the far field where  $(\xi, \eta) \sim (\log r, \theta)$ , this basic state consists of flow associated with a circular vortex (the term proportional to  $\xi$ ) and flow associated with a wave of wavenumber 2 on that vortex [the term proportional to  $\exp(-2\xi) \cos 2\eta$ ]. The streamfunction within the vortex is more conveniently expressed in Cartesian coordinates; thus, for  $\hat{x}^2/a^2 + \hat{y}^2/b^2 \leq 1$ ,

$$\bar{\psi} = \frac{\bar{\zeta}}{2(a + b)} (bx^2 + ay^2). \tag{13b}$$

Since the vortex rotates without change of shape, the time dependence of  $\bar{\psi}$  is obtained by replacing  $(x, y)$  in (13b) and (14) with the rotating coordinates

$$\begin{aligned} \hat{x} &= x \cos \bar{n}t + y \sin \bar{n}t, \\ \hat{y} &= -x \sin \bar{n}t + y \cos \bar{n}t. \end{aligned} \tag{15}$$

Now consider an initial perturbation that changes the vorticity within the ellipse from  $\bar{\zeta}$  to  $\bar{\zeta} + \zeta'$ , but leaves the shape of the ellipse unchanged. The evolution of this perturbation could be calculated, as for (5), explicitly from the linearized vorticity equation (3). In this case, however, it is more convenient to note that (12) and (13) are valid for any  $\bar{\zeta}$  and to Taylor expand  $\bar{\psi}$  as a function of  $\bar{\zeta}$ .

If quadratic terms in  $\zeta'$  are neglected, the perturbation is then

$$\psi' = \bar{\psi}(\bar{\zeta} + \zeta') - \bar{\psi}(\bar{\zeta}) = \zeta' \frac{\partial \bar{\psi}}{\partial \bar{\zeta}}. \tag{16}$$

Taking a  $\bar{\zeta}$  derivative of (13) and using (12), (14), and (15) to determine the dependence of  $(\xi, \eta)$  on  $\bar{\zeta}$  gives

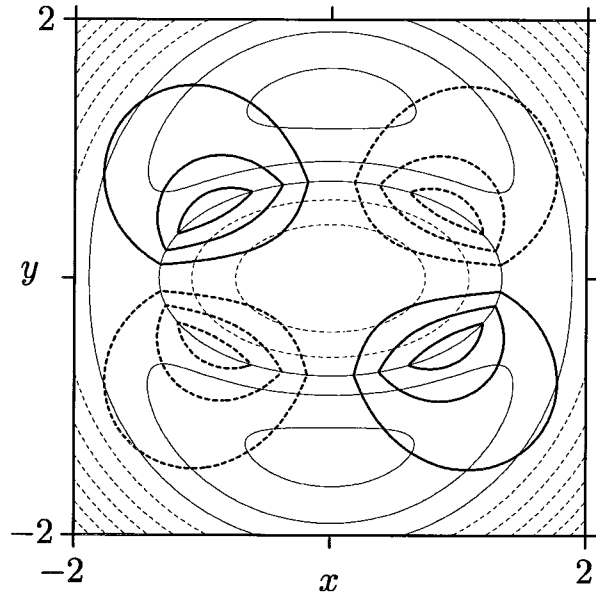


FIG. 1. Streamfunction  $\bar{\psi}$  for the flow relative to the elliptical vortex with  $a = 4/3$  and  $b = 3/4$  (thin lines; negative values dashed), and the portion of  $\psi'$  in (17) proportional to  $t$  (bold lines; zero contour suppressed). Contour intervals are 0.038 for  $\bar{\psi}$  and 1/4 the maximum of  $\psi'$ . Note that  $\bar{\psi} = 0$  is chosen on the boundary  $x^2/a^2 + y^2/b^2 = 1$  of the vortex.

$$\begin{aligned} \psi' &= \frac{1}{4} ab \zeta' \left[ 2\xi + e^{-2\xi} \cos 2\eta + \frac{\bar{n}t \sin 2\eta}{\cos^2 \eta - \cosh^2 \xi} \right. \\ &\quad \left. \times (1 - e^{-2\xi} (\cos 2\eta + \sinh 2\xi)) \right], \end{aligned} \tag{17a}$$

for  $\cosh \xi \geq a/d$ , where  $(\xi, \eta)$  are understood to be functions of  $(\hat{x}, \hat{y})$ ; and

$$\psi' = \frac{\zeta'}{2(a + b)} \left[ a\hat{x}^2 + b\hat{y}^2 + \frac{2\bar{\zeta}ab(b - a)}{(a + b)^2} t\hat{x}\hat{y} \right], \tag{17b}$$

for  $\hat{x}^2/a^2 + \hat{y}^2/b^2 \leq 1$ . Figure 1 displays streamlines relative to the basic-state vortex and contours of that part of  $\psi'$  in (17) proportional to  $t$ .

The perturbation is the sum of time-independent terms (in coordinates rotating with the basic-state vortex) and terms that increase linearly with  $t$ . The time-independent terms correspond to the flow associated with the initial vorticity perturbation and have the same form as the basic state (13). Much as in the previous examples, the portion of  $\psi'$  that grows linearly in  $t$  varies as  $\sin 2\eta$  and thus is phase shifted “downstream” (i.e., in the same sense as the flow associated with the perturbation vorticity) by roughly a quarter-wavelength relative to the basic-state wave, which varies as  $\cos 2\eta$ . Unlike the previous examples, the perturbation also contains higher harmonics that increase linearly in  $t$ .

The growth of the perturbation as a phase error once again arises because of changes to the medium for the finite-amplitude waves. In this case, perturbing the vor-

ticity in the ellipse changes the vorticity jump at the vortex edge and thus the phase speed of the waves. A similar calculation yields the behavior of a perturbation that alters the amplitude of the basic-state wave; such perturbations correspond to varying, say,  $a$  while leaving  $ab$  and  $\bar{\zeta}$  fixed. The perturbation solution then consists of time-independent terms corresponding to flow associated with a small change in  $a$  and terms proportional to  $t$  that have the same spatial structure as those in (17). In this case, the growing phase error arises from the dependence, through (12), of the rotation rate of the vortex on  $a$ .

*c. A heuristic treatment of growing basic-state waves*

Let the basic state consist of a finite-amplitude wave of the form

$$\bar{\psi} \sim \bar{\psi}_0 \operatorname{Re}[e^{ik(x-\bar{c}t)}] = \bar{\psi}_0 \exp(k\bar{c}_i t) \operatorname{cosk}(x - \bar{c}_r t),$$

superposed on a time-independent medium. Suppose now that the medium is perturbed in such a way that the wave's phase speed becomes  $c = \bar{c} + c'$ , where  $|c'/\bar{c}| \ll 1$ .

Considering  $\bar{\psi}$  as a function of  $\bar{c}$ , the reasoning leading to (16) then implies

$$\begin{aligned} \psi' &= \bar{\psi}_0 \operatorname{Re} \left( c' \frac{\partial \bar{\psi}}{\partial \bar{c}} \right) \\ &\sim \bar{\psi}_0 k t \exp(kc_i t) [c'_i \operatorname{cosk}(x - \bar{c}_r t) \\ &\quad + c'_r \operatorname{sink}(x - \bar{c}_r t)]. \end{aligned}$$

Small perturbations therefore again grow as  $t$  multiplied by time dependence inherited from the basic-state wave, which here includes both propagation and growth. The phase of  $\psi'$  relative to the basic-state wave depends on the magnitudes of the modifications to growth and propagation of the basic state; if modifications to the growth rate dominate modifications to the propagation ( $c'_i/c'_r \gg 1$ ),  $\psi'$  is nearly in phase with  $\bar{\psi}$  and serves to correct the amplitude of  $\bar{\psi}$ , while if modifications to the propagation dominate,  $\psi'$  is a quarter-wave-length out of phase with  $\bar{\psi}$  as in the previous examples. Note also that a finite-amplitude basic-state wave is required for growth, since the perturbation growth scales as the initial amplitude  $\bar{\psi}_0$  of the parent wave.

**4. Perturbations to a vortex dipole**

In addition to finite-amplitude waves, atmospheric flows often contain localized vortical structures. A barotropic vortex dipole on an  $f$  plane is a simple example of such a structure and will be considered below. Similar solutions generalized to baroclinic flows and the  $\beta$  plane (e.g., Flierl et al. 1980) are sometimes termed "modons."

Consider a distribution of relative vorticity confined to the disk  $r < R$ , with positive relative vorticity on one

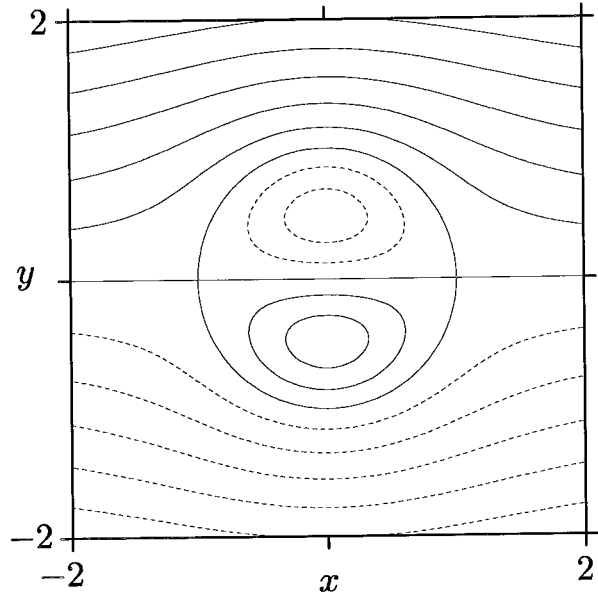


FIG. 2. Streamfunction  $\bar{\psi}$  for the flow relative to the dipole vortex given by (18) with  $R = U = 1$ . Contour interval is 0.3 and negative contours are dashed.

side of a diameter of the disk and negative relative vorticity on the other. Because of the antisymmetry of the vorticity distribution, this eddy will tend to propagate; we seek a solution that propagates steadily at speed  $U$ .

In this example, we will work exclusively in coordinates moving with the vortex dipole, whose motion may be taken to be along the  $x$  axis. The solution is again given by Lamb (1945, art. 165); the streamfunction is

$$\bar{\psi} = \begin{cases} CJ_1(\kappa r) \sin\theta, & r < R; \\ U \left( r - \frac{R^2}{r} \right) \sin\theta, & r > R. \end{cases} \quad (18)$$

The amplitude  $C$  of the interior streamfunction is related to  $U$  by  $2U = \kappa CJ_0(\kappa R)$ , the constant  $\kappa$  satisfies  $J_1(\kappa R) = 0$ , and  $J_0$  and  $J_1$  are Bessel functions of the first kind of orders 0 and 1. Figure 2 shows  $\bar{\psi}$ . Note that  $\psi \sim Uy$  as  $r \rightarrow \infty$ , consistent with the propagation of the dipole along the  $x$  axis at speed  $U$ .

Now suppose that a perturbation is added to the dipole, with uniform vorticity  $\zeta'_0$  in the disk  $r < R$  and zero vorticity elsewhere. Advection of the dipole by the perturbation flow will produce a rotation of the dipole that increases linearly with  $t$ . As the dipole rotates, it will propagate with a component of velocity normal to its original trajectory. The displacement of the dipole from its unperturbed position should increase as  $t^2$ , since the rotation is linear in  $t$ .

This suggests a perturbation solution of the form

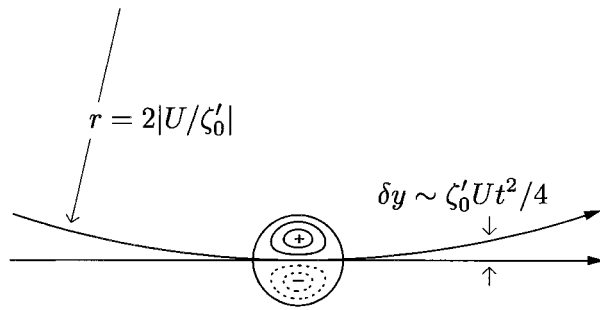


FIG. 3. Propagation of a dipole vortex perturbed by a disturbance with uniform vorticity. The unperturbed dipole, whose vorticity field is shown in the center of the figure, moves from left to right at speed  $U$  along the straight horizontal path. Adding uniform vorticity  $\zeta'_0$  over the disk of the dipole (and zero vorticity elsewhere) results in the dipole moving at the same speed along the circle of radius  $r = 2|U/\zeta'_0|$  tangent to the original path and with fixed orientation relative to the center of the circle. When  $\zeta'_0 t \ll 1$ , the perturbed dipole is displaced a distance of  $\zeta'_0 U t^2/4$  perpendicular to the original path.

$$\psi' = \begin{cases} \frac{1}{4}\zeta'_0[r^2 + at(\bar{\psi}_\theta + Ur \cos\theta) + bt^2\bar{\psi}_y], & r < R; \\ \frac{1}{4}\zeta'_0[R^2 \log(r/R) + atUr^{-1} \cos\theta \\ + bt^2U(r/R)^{-2} \cos 2\theta], & r < R. \end{cases} \quad (19)$$

For  $r < R$ , the terms in  $t\bar{\psi}_\theta$  and  $t^2\bar{\psi}_y$  represent the rotation and  $y$  displacement, respectively, of the dipole; the other terms in (19) are required for continuity of  $\psi'$  and its derivatives at  $r = R$ . Substitution of (18) and (19) into (3) shows that  $a = 2$  and  $b = U$ . This solution demonstrates that errors in the position of a feature may have complicated time dependence (other than proportional to  $t$ ) even with linearized dynamics.

As in the previous examples, (19) is a small-amplitude or short-time approximation to the difference between two known nonlinear solutions. Adding constant vorticity to the dipole results in an “eddy” that moves at the same speed as the original dipole but along a circle of radius  $2|U/\zeta'_0|$ . [This trajectory results from the fact that the quantities  $X = \int x\zeta \, dx \, dy / \int \zeta \, dx \, dy = 0$  and  $Y = \int y\zeta \, dx \, dy / \int \zeta \, dx \, dy = 2U/\zeta'_0$  are constants of the motion (Lamb 1945; art. 154).] Comparing the two solutions for short times, differences are a rotation of the dipole that increases as  $t$  and a displacement of the center of the eddy increasing as  $t^2$ , as shown schematically in Fig. 3.

## 5. Summary and discussion

In thinking about the growth of small perturbations in complex atmospheric flows, one is tempted to begin with barotropic and baroclinic instabilities of steady parallel flows and then to generalize those instabilities to nonparallel and time-dependent flows. Conceptually, such a generalization rests on an implicit assumption, as in WKB methods, that variations of the basic state

are sufficiently slow that insights from parallel or steady flows are locally useful. An alternative scenario, outlined here, is for perturbations to grow as errors in the position or amplitude of finite-amplitude features that are present already in the flow. Thus, while the canonical problem in baroclinic instability is the growth of waves on a zonal jet, an analogous problem for the growth of phase errors might start with a wavy jet as a basic state and perturb the wave amplitude or the zonal average.

The foregoing examples demonstrate the variety of basic states supporting perturbations that grow as phase errors. The linearized perturbation growth is algebraic in  $t$ , except for the case of a growing basic-state wave (section 3c), and is unbounded, rather than transient, in all the examples. When the basic state is a finite-amplitude barotropic Rossby wave, phase errors have amplifications smaller than but comparable to the optimal amplification [as calculated by Yoden and Nomura (1993)] for time intervals shorter the basic-state advective timescale. For longer time intervals, phase errors account for the most rapidly amplifying perturbations. All the examples have the property that the timescale for growth is the advective timescale for the basic-state wave or coherent structure.

In each example, the perturbation solution is the short-time and small-perturbation limit of the difference between two known nonlinear solutions. Both the growth and eventual “nonlinear saturation” of the perturbations are most easily understood through these nonlinear solutions, rather than through the linearized, perturbation equations.

Although no evidence is presented here, it seems likely that these results generalize to more complex flows. That is, initial perturbations to the location, amplitude, or structure of preexisting features, or to the medium in which they are embedded, will also grow in more complex flows.

In applying these results to forecast errors, one question that arises is whether the linearized solutions are valid, for initial errors of the magnitude expected in operational analyses, on the basic-state advective timescale over which the phase errors grow. Atmospheric motions of synoptic or larger scales are characterized by advective timescales of one to a few days. The forecast range over which error evolution can be approximated by linearized dynamics varies but generally extends to 48 h (Errico et al. 1993). The timescale for the growth of phase errors is thus comparable to the timescale over which linearized evolution of errors is valid. Note, in addition, that the growth of phase errors in the examples is not limited to the linear regime.

A remaining question is the importance of this scenario relative to other mechanisms for error growth. The most rapidly growing errors in present global forecasts typically resemble finite-time barotropic–baroclinic instabilities, rather than phase errors, in their initial structure (Buizza and Palmer 1995). The same numerical forecasts, however, also routinely support rapidly grow-

ing perturbations that are *not* obvious analogs of finite-time baroclinic instabilities (see Figs. 16, 17 of Buizza and Palmer). Moreover, for certain basic states and norms, phase errors are clearly the fastest growing errors. For example, phase errors maximize the growth of perturbation energy or enstrophy within idealized finite-amplitude baroclinic waves (Snyder and Joly 1998).

In addition, forecast errors are often errors in the phase or amplitude of existing features (e.g., Hawes and Colucci 1986). This fact suggests that the growth of phase errors, while perhaps not dominant, does exert some influence on forecast errors, with the result that errors are tied to existing features in the forecast. Indeed, even when the most rapidly growing perturbations appear to be finite-time baroclinic instabilities, their evolved structure often represents an error in the position or amplitude of a preexisting feature. Ehrendorfer and Errico (1995) show one example.

Thus, available evidence suggests a role for phase errors in the growth of forecast error or, more generally, in perturbation growth in complex flows. Given the above considerations, the mechanism presented here may not be the dominant source of error growth except in specialized cases. At the same time, its contributions cannot easily be discounted (say, on the basis of energetics).

The role of phase errors averaged over many forecasts also undoubtedly depends on the statistics of the initial or analysis errors. If, for example, the highly tilted initial structure of finite-time barotropic–baroclinic instabilities is unlikely to occur in the initial errors, one expects such instabilities to contribute proportionally less to error growth. [A related issue is the preferred choice of norm for the calculation of optimal perturbations or singular vectors; see Houtekamer (1995) and Palmer et al. (1998).] Calculations that account for the statistics of analysis errors reveal dominant errors that have a larger scale, smoother horizontal and vertical structure, and reduced growth rates (Barkmeijer et al. 1998). Answers from these calculations, however, are not yet definitive, as the estimates of analysis error covariances used are crude.

*Acknowledgments.* Enjoyable discussions with C. Bishop and Z. Toth stimulated my interest in this problem. R. Rotunno assisted with the analytic solutions.

## APPENDIX

### Explicit Form of (7)

Let us nondimensionalize lengths by  $k^{-1}$ , time by  $k\beta^{-1}$ , and streamfunction by  $k^{-3}\beta$ , and set  $l = k$  as in Yoden and Nomura (1993). Yoden and Nomura expand  $\psi'$  for  $0 \leq x \leq 2\pi$  and  $0 \leq y \leq \pi$  in terms of the basis functions  $\cos my$ ,  $\sin my \sin nx$ , and  $\sin my \cos nx$ . They truncate the expansion beyond  $m = n = 8$ .

In analogy to (5), we seek a solution to the truncation of (3) of the form

$$\psi' = A[\eta(y) + i\bar{\psi}_x], \quad (\text{A1})$$

where  $A$  is an arbitrary nondimensional constant and

$$\eta(y) = \sum_{m=1}^8 a_m \cos my.$$

If (A1) were a solution without truncation, (3) would imply

$$-2\bar{\psi}_x = \bar{\psi}_x(\nabla^2 + 2)\eta_y,$$

or equivalently,

$$2 \sin y = \sin y(\nabla^2 + 2) \sum_{m=1}^8 m a_m \sin my. \quad (\text{A2})$$

In a truncated model, (A2) requires coefficients of the spectral expansions of each side of the equation to agree up to, but not beyond, the truncation. Multiplying (A2) by  $\sin ny$  ( $n = 1, \dots, 8$ ) and integrating over the domain then yields eight equations in the unknowns  $\{a_m; m = 1, \dots, 8\}$ . The solution is  $a_m = 0$  for  $m$  even, and

$$a_1 = 0.843, \quad a_3 = 0.024, \quad a_5 = 0.003, \\ a_7 = 0.006.$$

## REFERENCES

- Barkmeijer, J., M. van Gijzen, and F. Bouttier, 1998: Singular vectors and the analysis error covariance metric. *Quart. J. Roy. Meteor. Soc.*, **124**, 1695–1713.
- Borges, M. D., and D. L. Hartman, 1992: Barotropic instability and optimal perturbations of observed nonzonal flows. *J. Atmos. Sci.*, **49**, 335–354.
- Buizza, R., and T. N. Palmer, 1995: The singular-vector structure of the atmospheric general circulation. *J. Atmos. Sci.*, **52**, 1434–1456.
- Ehrendorfer, M., and R. M. Errico, 1995: Mesoscale predictability and the spectrum of optimal perturbations. *J. Atmos. Sci.*, **52**, 3475–3500.
- Errico, R. M., T. Vukicevic, and K. Raeder, 1993: Examination of the accuracy of a tangent linear model. *Tellus*, **45A**, 462–477.
- Farrell, B., 1985: Transient growth of baroclinic waves. *J. Atmos. Sci.*, **42**, 2718–2727.
- , 1989: Transient development in confluent and diffluent flow. *J. Atmos. Sci.*, **46**, 3279–3288.
- Flierl, G. R., V. D. Larichev, J. C. McWilliams, and G. M. Reznik, 1980: The dynamics of baroclinic and barotropic solitary eddies. *Dyn. Atmos. Oceans*, **5**, 1–41.
- Gill, A. E., 1982: *Atmosphere–Ocean Dynamics*. Academic Press, 662 pp.
- Hawes, J. T., and S. T. Colucci, 1986: An examination of 500-mb cyclones and anticyclones in National Meteorological Center prediction models. *Mon. Wea. Rev.*, **114**, 2163–2175.
- Houtekamer, P. L., 1995: The construction of optimal modes. *Mon. Wea. Rev.*, **123**, 2888–2898.
- Lamb, H., 1945: *Hydrodynamics*. 6th ed. Dover, 738 pp.
- Palmer, T. N., R. Gelaro, J. Barkmeijer, and R. Buizza, 1998: Singular vectors, metrics, and adaptive observations. *J. Atmos. Sci.*, **55**, 633–653.
- Snyder, C., and A. Joly, 1998: Development of perturbations within a growing baroclinic wave. *Quart. J. Roy. Meteor. Soc.*, **124**, 1961–1983.
- Yoden, S., and M. Nomura, 1993: Finite-time Lyapunov stability analysis and its application to atmospheric predictability. *J. Atmos. Sci.*, **50**, 1531–1543.